Environmental Science
Water Research & Technology

ROYAL SOCIETY OF CHEMISTRY

PAPER

View Article Online
View Journal | View Issue

Cite this: *Environ. Sci.: Water Res. Technol.*, 2021, **7**, 1971

The adsorption of phytate onto an Fe–Al–La trimetal composite adsorbent: kinetics, isotherms, mechanism and implication

Yuanrong Zhu,[a] Zhan Liu,[b] Kun Luo,[b] Fazhi Xie,*[b] Zhongqi He,[c] Haiqing Liao[a] and John P. Giesy[adef]

Phytate is the most abundant organic phosphorus (P) in the environment and is also an important bioavailable P source for algal blooms in some lakes. A novel Fe–Al–La (FAL) tri-metal composite adsorbent was developed by the coprecipitation method. The maximum adsorption capacity was 2.09 μmol m^{-2} at 298 K and an initial pH of 4.0, and it could keep high adsorption capacity when the pH varied from 4.0 to 9.0. The dominant process for the adsorption of phytate by the FAL adsorbent was surface chemical reactions mainly by monolayer coverage. The adsorption was best described by Langmuir isotherms, and its kinetics by a pseudo-second-order kinetic equation. Thermodynamic parameters indicated that adsorption of phytate by the FAL adsorbent was a spontaneous and endothermic process. The adsorption capacity decreased with pH variation from 3.2 to 11.0, especially when pH > 9.0. The sequence of strength of competition of coexisting anions with phytate was CO_3^{2-} > SO_4^{2-} > NO_3^- > Cl^-. Dissolved organic matter (DOM) also competed for adsorption sites with phytate on the surface of the FAL adsorbent. Fourier transform infrared (FT-IR) spectroscopic and X-ray photoelectron spectroscopic (XPS) analyses showed that phytate had been adsorbed onto the surface of the FAL adsorbent and that Fe, Al and La all participated in adsorption. The prepared FAL adsorbent exhibited potential for removing both phytate and other phosphate species during treatment of wastewaters including those from pig and poultry manures. The FAL adsorbent could also be a potential agent for immobilization of both phytate and phosphate in overlying water and lake sediments. This study also indicated that eutrophication of lakes would increase the potential of phytate to be a bioavailable form of P in blooming of algae.

Received 7th May 2021,
Accepted 16th August 2021

DOI: 10.1039/d1ew00318f

rsc.li/es-water

Water impact

Phytate is the most abundant organic phosphorus (P) species in the environment, which is widely present in wastewater, soils, sediments and poultry litter and is also an important bioavailable P source for algal blooms in lakes. The adsorbent with a high adsorption capacity would be important for recovery or immobilization of phytate from wastewater, soils, sediments and poultry litter. The adsorption and desorption mechanisms of phytate onto Fe and Al oxides are also fundamental processes in understanding the biogeochemical cycling of phytate in water, soils or sediments.

1 Introduction

Phosphorus (P) is an element that is a nutrient essential for life and a major contributor to nonpoint-source pollution and eutrophication.[1] Thus, biogeochemical cycling of P and methods to reduce and control P in wastewater, natural water, and sediments have been widely studied.[2–5] The predominant inorganic P species such as HPO_4^{2-} or $H_2PO_4^-$ are the most bioavailable forms of P, and emphasis has been placed on the study of inorganic P abundance, dynamics, adsorption and desorption by various adsorbents for many decades.[6] However, in most wastewater, natural water, soils, sediments and manure, organic P in the form of phytate, nucleic acids, phospholipids, sugar phosphates, and organic condensed P species is at least as abundant as inorganic P. In particular, phytate, which is the most abundant organic P in the environment,[7] is widely present in wastewaters,[8] soils,[9–11] sediments[12,13] and poultry litter.[14,15] Additionally,

[a] *State Key Laboratory of Environmental Criteria and Risk Assessment, Chinese Research Academy of Environmental Sciences, Beijing 100012, China*
[b] *School of Materials Science and Chemical Engineering, Anhui Jianzhu University, Hefei 230601, China. E-mail: fzxie@mail.ustc.edu.cn*
[c] *USDA-ARS, Southern Regional Research Center, 1100 Robert E Lee Blvd, New Orleans, LA 70124, USA*
[d] *Toxicology Centre, University of Saskatchewan, Saskatoon, Saskatchewan, Canada*
[e] *Department of Veterinary Biomedical Sciences and Toxicology Centre, University of Saskatchewan, Saskatoon, Saskatchewan, Canada*
[f] *Department of Environmental Sciences, Baylor University, Waco, Texas, USA*

phytate is likely an important bioavailable P source for algal blooms in some lakes, such as Lake Dianchi, China.[3]

Phytate with six phosphate groups linked to the six carbon atoms of the inositol ring has a highly negative charge and can strongly interact with metal ions and metal oxides such as aluminum (Al) and iron (Fe) oxides.[16,17] The adsorption and desorption of phytate by various monometallic oxide-based adsorbents such as Al_2O_3,[18,19] hematite,[20] goethite,[21] and kaolinite[22,23] have been reported. Compared to orthophosphate, phytate is not only much larger in molecular size and structure, but also possesses much more complex functional groups and shows very different pronation and depronation characteristics.[24] Thus, the adsorption characteristics (rate, affinity, capacity, and binding mode) of phytate and orthophosphate are rather different.[19,24–26] However, previous studies have mainly focused on monometallic oxides and have paid little attention to binary metal oxides or trimetallic oxides.[27,28] Phytate can form complexes with Fe and Al oxides,[22,29] and can also precipitate on surfaces of Fe and Al oxides.[19,30] Fe and Al oxides are important for the precipitation, adsorption, desorption and bioavailability of phytate in soils[22,29] and sediments.[31,32] Thus, the adsorption and desorption mechanisms of phytate onto Fe and Al oxides are fundamental processes in understanding the biogeochemical cycling of phytate or effective control of redundant phytate in water, soils or sediments. Indeed, it is proposed that phytate found in animal manure has a strong chelating ability with metal ions with potential for *in situ* immobilization of heavy metals and remediation of metal-contaminated soils.[33]

Lanthanum (La) is known to have high affinity for some anions, such as phosphate and fluoride,[5,34,35] and is also relatively abundant in the Earth's crust. However, the price of La is higher than that of some other metals, such as magnesium (Mg), Al, and Fe. Thus, La oxide is usually combined with other metal oxides to form La-type adsorbents, such as La–Fe binary oxides,[36] La–Mg–Fe trimetal oxides,[37] and La–Fe–Mn trimetal oxides.[34] In this study, a novel Fe–Al–La (FAL) trimetal composite adsorbent that is less costly to produce than La oxide alone and is also more environmentally friendly was developed. Phytate adsorption experiments including measurement of adsorption kinetics, adsorption isotherms, thermodynamic parameters, and the effects of pH, anions, and dissolved organic matter (DOM) on the FAL adsorbent were performed. The mechanisms of adsorption of phytate by the FAL adsorbent are analyzed and discussed. Finally, the potential application of the prepared FAL adsorbent for environmental remediation and implications for the migration and transformation of phytate in lakes are also discussed.

2 Materials and methods

2.1 Materials

Analytical reagent grade chemicals, including $Fe(NO_3)_3{\cdot}9H_2O$, $La(NO_3)_3{\cdot}6H_2O$, $Al(NO_3)_3{\cdot}9H_2O$, NaOH, HCl, and $NaNO_3$, were purchased from Shanghai Macklin Biochemical Co., Ltd (Shanghai, China). Humic acid (HA, CAS: 1415-93-6, Sigma No. 53680) and phytate ($C_6H_{18}O_{24}P_6{\cdot}xNa^+{\cdot}yH_2O$, analytical reagent grade, CAS: 14306-25-3, Sigma No. P8810) were both purchased from Sigma-Aldrich Trading Co., Ltd (Shanghai, China).

A stock solution of phytate (1000 mg P L^{-1}) was prepared by dissolving an appropriate quantity of phytate in ultrapure water in a 1 L volumetric flask. In the same way, stock solutions of $NaNO_3$ (0.5 mol L^{-1}) and HA (500 mg C L^{-1}) were prepared.

2.2 Sorbent preparation

The FAL adsorbent with an Fe : Al : La molar ratio of 2 : 2 : 1 was prepared by a coprecipitation method.[38,39] The ratio was decided based on our preliminary result as well as the consideration of the material cost. Briefly, the working solutions of $Fe(NO_3)_3$, $Al(NO_3)_3$, and $La(NO_3)_3$ were diluted from their corresponding stock solution to 0.2 mol L^{-1}, 0.2 mol L^{-1} and 0.1 mol L^{-1}, respectively. These solutions were then combined. Sodium hydroxide solution (1 mol L^{-1}) was then added to the mixed solution until the pH approached 9.0. The solution was continuously mixed for 1 h with a magnetic stirrer. The Fe–Mn–La precipitate was aged for 24 h at room temperature. Then, the precipitate was washed several times with ultrapure water. The precipitate was filtered and dried in an oven at 338 K for 24 h. Finally, the dried FAL trimetal material was ground into a fine powder and kept in a dessicator at room temperature for subsequent analyses.

2.3 Characterization of adsorbents and humic acid

The purchased HA was characterized by UV-visible spectrophotometry (Agilent 8453), Fourier transform infrared (FT-IR) spectroscopy (Nicolet 6700, Thermo Scientific), and three dimensional fluorescence spectrometry (Cary Eclipse, Agilent).

The zeta potential of the prepared FAL adsorbent was analyzed. First, the prepared 0.5 mol L^{-1} NaCl solution was added to five 50 mL centrifuge tubes. The initial pH ranged from 3.0 to 11.0. The FAL adsorbent (1 g L^{-1}) was added to these centrifuge tubes and incubated for 24 h. The final pH remained at 3.2, 5.2, 7.0, 9.0, or 11.0. Zeta potential was measured by the use of a zeta potential analyzer (Malvern Zetasizer Nano-ZS). In order to analyze the porosity and specific surface area of the prepared FAL sorbent, nitrogen adsorption/desorption isotherms were measured using an ASAP 2020 M surface area and porosity analyzer (Micromeritics Instruments Crop., USA).

The prepared FAL adsorbent was characterized by X-ray diffraction (XRD, Bruker D8 Advance, Bruker AXS, Germany). The FAL adsorbent was analyzed by FT-IR spectroscopy (Nicolet 6700, Thermo Scientific), before and after adsorption of phytate. X-ray photoelectron spectroscopy (XPS) analysis of

the FAL adsorbent after phytate adsorption was performed with an ESCALAB 250 instrument (Thermo Fisher VG).

2.4 Adsorption experiments

2.4.1 Adsorption kinetics. Adsorption kinetics was investigated at an initial phytate concentration of 10 mg P L^{-1} with a background ionic strength of 0.01 mol L^{-1} $NaNO_3$. In addition, the initial pH of the solution was controlled at 4.0 ± 0.2 *via* addition of an acid or base. FAL adsorbents (20 mg) were added to 50 mL centrifuge tubes. These centrifuge tubes were then shaken at 298 K. The samples were incubated for specific durations from 0 to 60 h. That is, at a specific incubation interval, triplicate tubes of the incubation mixtures were centrifuged and the subsequent supernatants were further filtered. Phosphorus in these clean supernatants was determined by the molybdenum blue/ascorbic acid method[40] after $K_2S_2O_8$ digestion.

2.4.2 Adsorption isotherms. The procedure of the adsorption isotherm experiment was similar to that of the adsorption kinetics experiment, but the variables were the concentration of phytate and incubation temperature, rather than the incubation time. The concentration of phytate, calculated as phosphorus, was varied from 5 to 80 mg P L^{-1}. The working solutions were shaken until adsorption equilibrium was reached, which was determined by adsorption kinetic experiments. Three temperatures, 298, 308, and 318 K, were applied during adsorption equilibrium testing. These solutions were then centrifuged and filtered for clean supernatants, and the phytate concentration remaining in the supernatants was determined by the use of the molybdenum blue method after digestion of samples with $K_2S_2O_8$. The amount of adsorbed phytate was calculated by the difference in phytate concentration, calculated as phosphorus, measured before and after adsorption equilibrium was reached.

2.4.3 Influencing factors. The impacts of the selected influencing factors on adsorption were evaluated under the optimal incubation conditions determined in subsections 2.4.1 and 2.4.2. These selected factors included pH, anions including CO_3^{2-}, SO_4^{2-}, Cl^-, and NO_3^-, dissolved organic matter (represented by HA), and content of the FAL adsorbent itself. A series of phytate solutions (10 mg P L^{-1}) with initial pH from 3.0 to 11.0 and a background ionic strength of 0.01 mol L^{-1} $NaNO_3$ were prepared.

Phytate solutions with a range of ionic strengths including 0.01, 0.05, and 0.1 mol L^{-1} were also prepared. The initial pH was maintained at 4.0 ± 0.2 *via* addition of an acid or base. Subsequent adsorption experiment steps were the same as previously described.

A series of phytate solutions (20 mg P L^{-1}) with various concentrations of HA (10 to 100 mg C L^{-1}) were prepared. The initial pH was maintained at 4.0 ± 0.2 *via* addition of an acid or base and the ionic strength was maintained at 0.01 mol L^{-1} $NaNO_3$. Subsequent adsorption experiment steps were the same as previously described.

Various amounts of the FAL adsorbent from 10 to 50 mg were added to 50 mL centrifuge tubes and then 50 mL of phytate solution (10 mg P L^{-1}) was added to the centrifuge tubes. The initial pH was maintained at 4.0 ± 0.2 *via* addition of an acid or base and the ionic strength was 0.01 mol L^{-1} $NaNO_3$. Subsequent adsorption experiment steps were the same as previously described.

2.5 Analysis of data

2.5.1 Adsorption capacity and removal efficiency. The adsorption capacity and removal efficiency were calculated (eqn (1)).

$$q_e = \frac{(C_0 - C_t)V}{m} \quad (1)$$

where q_e is the equilibrium adsorption capacity (mg g^{-1}), C_0 is the initial concentration (mg L^{-1}) of the adsorbent, C_t is the adsorbent concentration at time t (mg L^{-1}), V is the volume of the solution (mL), and m is the weight of the adsorbent (g).

2.5.2 Adsorption kinetics. The pseudo-first-order kinetic relationship (eqn (2)) and pseudo-second-order kinetic relationship (eqn (3)) were applied to describe the kinetics of adsorption.[41]

$$\ln(q_e - q_t) = \ln q_e - k_1 t \quad (2)$$

$$\frac{t}{q_t} = \frac{1}{k_2 {q_e}^2} + \frac{1}{q_e} t \quad (3)$$

where q_e (mg g^{-1}) and q_t (mg g^{-1}) are the amount of phosphate adsorbed per unit mass of adsorbent at equilibrium and time t, respectively; k_1 (min^{-1} or h^{-1}) is the pseudo-first-order rate constant; k_2 (g mg^{-1} min^{-1} or g mg^{-1} h^{-1}) is the second-order constant for adsorption.

2.5.3 Adsorption isotherms. Both the Langmuir (eqn (4)) and Freundlich relationships (eqn (5)) were used to describe adsorption:[42]

$$q_e = \frac{q_m K_L C_e}{1 + K_L C_e} \quad (4)$$

$$q_e = K_F {C_e}^{1/n} \quad (5)$$

where q_e is the equilibrium adsorption capacity (mg g^{-1}), C_e is the equilibrium liquid-phase concentration (mg L^{-1}), q_m is the theoretical saturation sorption capacity (mg g^{-1}), K_L is a constant related to the adsorption heat (L mg^{-1}), and K_F (mg^{1+n} L^n g^{-1}) and n are Freundlich constants.

2.5.4 Thermodynamic data. The thermodynamic parameters of the adsorption process were analyzed (eqn (6)–(8)):[43]

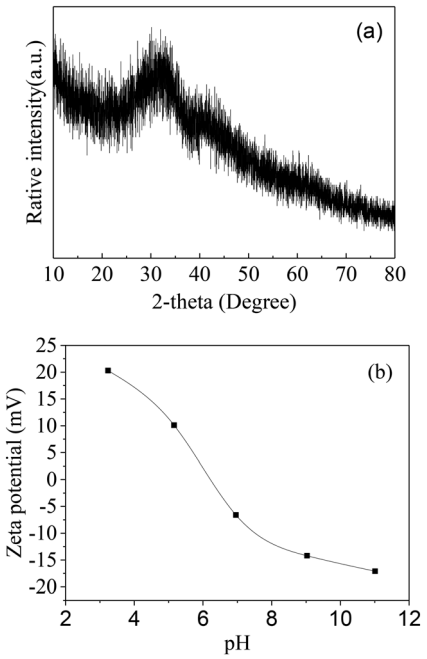

Fig. 1 XRD pattern (a) and zeta potential (b) of the Fe–Al–La trimetal adsorbent.

$$K_C = 55.5 \times 1000 \times K_L \quad (6)$$

$$\Delta G = -RT \ln K_C \quad (7)$$

$$\ln K_C = \frac{\Delta S}{R} - \frac{\Delta H}{R} \times \frac{1}{T} \quad (8)$$

where K_L is the Langmuir constant, K_c is the equilibrium constant, T is the absolute temperature (K), R is the gas constant (8.314 J mol^{-1} K^{-1}), ΔG^0 is the Gibbs free energy (kJ mol^{-1}), ΔH^0 is the change in enthalpy (kJ mol^{-1}), and ΔS^0 is the change in entropy (J mol^{-1} K^{-1}).

3 Results and discussion

3.1 Characterization of the FAL adsorbent and HA

When the crystal structure of the adsorbent was characterized by the use of XRD (Fig. 1a), no obvious characteristic peaks were observed, which indicated that the FAL adsorbent had an amorphous structure. Based on the zeta potential of the prepared FAL adsorbent (Fig. 1b), the pH at the point of zero charge (pH_{pzc}) of the FAL adsorbent was approximately 6.3. In other words, when the pH was less than 6.3, the functional groups on the adsorbent are positively charged, which created a favorable chemistry for the binding of negatively charged phytate. The surface charges of the FAL adsorbent became negative when the pH of the solution is above 6.3. Additionally, the prepared FAL adsorbent had a specific surface area of 68.1 m^2 g^{-1}. Additionally, more characterization of the prepared FAL adsorbent could be found in section 3.6, such as FT-IR and XPS spectra.

The UV-visible spectra of HA showed that the absorbance of HA decreased rapidly with increasing acquisition wavelength (Fig. 2a), typical for natural organic matter samples.[44] There were no obvious absorption peaks in the UV-visible spectra of HA. However, the prepared HA absorbed radiation significantly at wavelengths between 200 and 400 nm, which indicated that the majority of chromophores included aromatic groups with various degrees and types of substitution, such as polysubstituted and monosubstituted phenols and different aromatic acids.[45] The UV-visible eigenvalue of HA, *i.e.*, the ratio of absorbance at 250 nm to

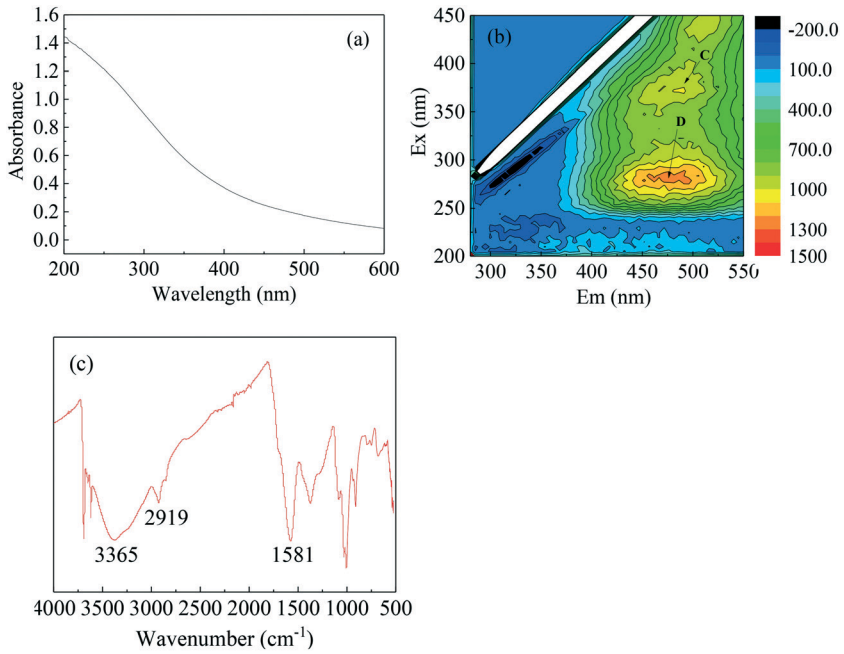

Fig. 2 UV-visible spectrum (a), three-dimensional fluorescence spectrum (b), and FT-IR spectrum (c) of humic acid.

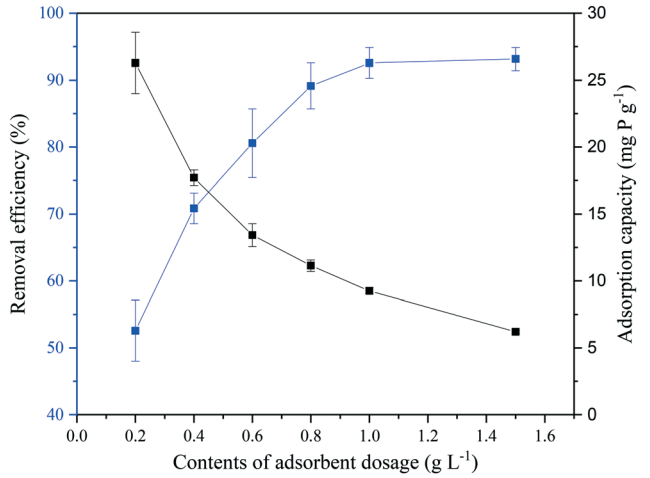

Fig. 3 Effect of the amount of adsorbent added on the removal efficiency and adsorption capacity (conditions: the initial concentration of phytate was 10 mg P L^{-1}, the initial pH was 4.0 ± 0.2, and the temperature was 298 K).

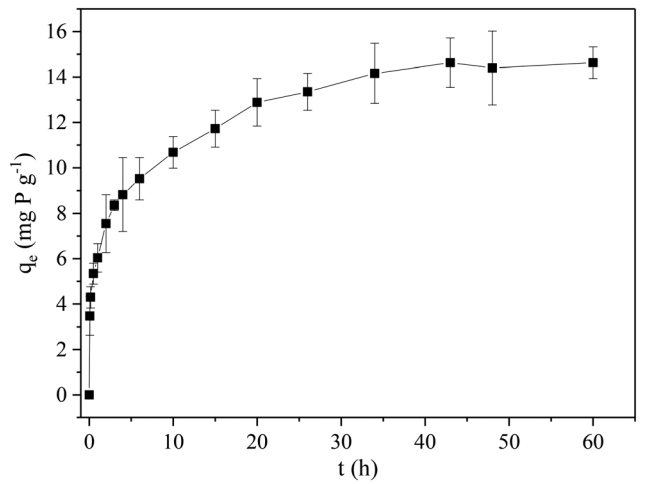

Fig. 4 Adsorption of phytate onto the Fe–Al–La trimetal adsorbent with time (the initial concentration was 10 mg P L^{-1}, temperature was controlled at 298 K, and the initial pH was controlled at 4.0 ± 0.2).

that at 365 nm (E_2/E_3), was 2.4, the ratio of absorbance at 300 nm to that at 400 nm (E_3/E_4) was 2.4, and the ratio of absorbance at 350 nm to that at 550 nm (E_3/E_5) was 4.8.

Additionally, peak C (Ex, 370 nm; Em, 480 nm) and peak D (Ex, 280 nm; Em, 475 nm) could be found in the excitation-emission matrix (EEM) spectrum of the prepared HA (Fig. 2b), and were typical characteristic peaks of HA.[46] The FT-IR spectrum of HA indicated some functional groups in the prepared HA (Fig. 2c). The band at approximately 1581 cm^{-1} could be attributed to C=C stretching in aromatic rings. The band at approximately 2919 cm^{-1} could be assigned to C–H stretching in aliphatic chains. The band centered at approximately 3365 cm^{-1} indicated the presence of OH groups.[47]

3.2 Adsorbent addition and adsorption kinetics

The efficiency of removal was directly proportional to the concentration of the FAL adsorbent from 0.2 to 1.5 g L^{-1}; however the adsorption capacity was decreased (Fig. 3). The efficiency of removal was approximately 93% at the steady state when the amount of adsorbent was approximately 1.0 g L^{-1}. When the amount of adsorbent added is low, the active sites would be fully exposed to the interactions with phytate, and the sites would be also saturated rapidly. High amounts of adsorbent would also provide enough sites for adsorption of phytate. Thus, the optimum adsorbent dosage could be checked by the concentration of phytate when the FAL adsorbent is applied. The adsorbent dosage of 0.4 g L^{-1} was applied in subsequent studies to characterize the adsorption of phytate and investigate the effect of other factors including the pH of solution, coexisting anions and DOM concentrations.

The adsorption of phytate by the FAL adsorbent was rapid with 37.7% of the initial phytate adsorbed within 0.5 h (Fig. 4). Then, 64.0% of the initial phytate was adsorbed by the FAL adsorbent within 8 h. After 8 h, due to the scarcity of available adsorption sites for phytate on the surface of the FAL sorbent, adsorption was significantly less, and the steady state was approached after approximately 32 h.

Adsorption kinetics were fitted with both pseudo-first-order and pseudo-second-order relationships (Table 1). Based on coefficient of determination (R^2) values, pseudo-second-order kinetics described the adsorption of phytate by the FAL adsorbent better. Also, theoretical adsorption capacities were predicted by the pseudo-first-order kinetic equation ($q_{e,1}$) and pseudo-second-order kinetic equation ($q_{e,2}$) (Table 1). The $q_{e,2}$ was consistent with the experimental data for the capacity for adsorption ($q_{e,exp}$). These results suggested that the surface chemical reactions between the active sites of the adsorbents and phytates are likely the dominant processes for the adsorption of phytates onto the FAL adsorbents.[48,49]

3.3 Adsorption isotherms and thermodynamics

Based on the adsorption isotherms of phytates onto the FAL adsorbent at the initial pH of 4.0 and at three different temperatures, the adsorption capacity increased significantly with the equilibrium concentration of phytate from 0 to 10

Table 1 Adsorption kinetic parameters of phytate onto the Fe–Al–La trimetal adsorbent

$q_{e,exp}$ (mg P g^{-1})	Pseudo-first-order			Pseudo-second-order		
	$q_{e,1}$ (mg P g^{-1})	K_1 (h^{-1})	R^2	$q_{e,2}$ (mg P g^{-1})	K_2 (g mg^{-1} h^{-1})	R^2
14.2	8.9	0.094	0.981	15.0	0.031	0.996

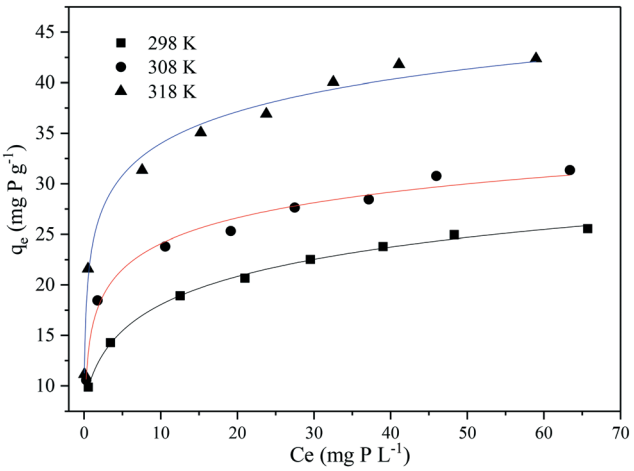

Fig. 5 Equilibrium isotherms of phytates onto the Fe–Al–La trimetal adsorbent at different temperatures.

mg P L^{-1} (Fig. 5). Saturation and equilibrium were achieved when the equilibrium concentration of phytate approached 60 mg P L^{-1}. The capacities for adsorption at the steady state were proportional to temperature (Fig. 5), which indicated that the adsorption of phytates by the FAL adsorbent was an endothermic process.[41]

When data were fitted to isotherms using Langmuir and Freundlich models, based on coefficients of determination (R^2), the Langmuir model best described the adsorption of phytates by the FAL sorbent at various temperatures ($R^2 >$ 0.993) (Table 2). This indicated that the adsorption of phytate by the FAL adsorbent is due to a surface monolayer.[50] Additionally, the values of K_L in the Langmuir model were all greater than 0, which indicated that the adsorption properties were excellent.[37]

The theoretical saturation sorption capacity (q_m) was 26.4, 31.9, and 43.0 mg g^{-1} at temperatures of 298, 308, and 318 K, respectively (Table 2). Based on the maximum sorption capacity and specific area of the adsorbent, the maximum adsorption densities for phytate by the FAL adsorbents were calculated. Under certain conditions, the maximum adsorption densities for phytate by the FAL adsorbents were greater than those of other Fe or Al adsorbents, except for the ferrihydrite–kaolinite adsorbents in the literature (Table 3). However, the adsorption capacity would also vary with different conditions for adsorption, such as the amount of adsorbent added, pH, and temperature. The adsorbent dosage was lowest for the FAL adsorbent in Table 3, which could lead to a higher adsorption capacity. Thus, it is difficult to conclude that the FAL adsorbent is truly better for adsorption of phytate. Generally, the FAL adsorbent has application potential for removal of phytate from water or for interrupting phytate release from sediments of lakes.

During adsorption, thermodynamic parameters, including ΔG^0, ΔH^0 and ΔS^0, were calculated from the adsorption isotherms of phytate on the FAL adsorbent at various temperatures (Fig. 5 and Table 4). Values for ΔG^0 varied from −29.4 to −15.1 kJ mol^{-1}, which indicated that the adsorption of phytate onto the FAL adsorbent was a spontaneous process.[51] Greater negative values of ΔG^0 were observed at higher temperatures, indicating that adsorption reactions were more thermodynamically favorable at higher temperatures than at relatively low temperatures. The positive ΔH^0 value (26.2 kJ mol^{-1}) indicated that this adsorption was an endothermic process. Additionally, the positive value of ΔS^0 (167.7 J mol^{-1} K^{-1}) suggested that the isothermal adsorption process of phytate onto the FAL adsorbent would increase the randomness at the solid–solution interface and the degree of disorder when phytate from the hydrous phase adsorbed onto the surface of the FAL adsorbent.[49,52]

3.4 Effects of pH

The capacities for adsorption at the steady state were proportional to the initial pH from 3.2 to 11.0 (Fig. 6a). When the initial pH was at 3.2, the initial concentration 10 mg P L^{-1} and the adsorbent concentration 0.4 g L^{-1}, the maximum proportion of phytate removed was 84.5%. The capacity for adsorption varied in a narrow range from 14. 2 to 11.4 mg P g^{-1} when the initial pH approached 4.0 to 9.0. However, the adsorption capacity would be decreased quickly after pH > 9.0. Generally, after adsorption of phytate onto the FAL adsorbent, the pH of solution varied in a narrow range. This implied that the prepared FAL adsorbent could be well applied in a wide pH of wastewater or overlying water of lakes ranging from 3.0 to 9.0. The capacities for adsorption were determined by the pH_{pzc} of the FAL adsorbent and forms of phytate in solutions.[34,53] Ionization and dissociation of dissolved phytate could be described in three steps such that ionization constants were 1.84, 6.30, and 9.70, respectively. In these three steps, 6, 2 and 4 H^+ ions are produced, respectively. Based on the ionization constants of dissolved phytate, species of phytate at different pH values were analyzed (Fig. 6b). And the pH_{pzc} of the FAL adsorbent was 6.3 (Fig. 1b). When the pH was <6.3, the species of dissolved phytate was electronegative, while the surface of the FAL adsorbent was positive. Thus, acidic conditions would be

Table 2 Langmuir and Freundlich isotherm parameters for phytate adsorption onto the Fe–Al–La trimetal adsorbent

Temperature (K)	Langmuir			Freundlich		
	q_m (mg P g^{-1})	K_L (L mg^{-1})	R^2	K_F (mg^{1+n} L^n g^{-1})	n^{-1}	R^2
298	26.4	0.272	0.994	11.151	0.205	0.998
308	31.9	0.367	0.993	14.674	0.191	0.968
318	43.0	0.529	0.995	21.309	0.181	0.980

Table 3 Comparison of the maximum adsorption capacities (calculated as sorption density by the maximum sorption capacity and specific area of the adsorbent) of phytate onto the Fe–Al–La adsorbent developed in this study and other adsorbents in previous studies

Adsorbent	Adsorbent dose (g L^{-1})	pH	Temperature (K)	pH_{pzc}	Adsorption capacity (μmol m^{-2})	Ref.
Nano γ-Al_2O_3	0.75	5.0	298	9.3	1.32	18
Ferrihydrite–kaolinite	2.75	4.5	298	6.5	2.24	22
Kaolinite	7.94	4.5	298	5.0	0.27	22
α-Al_2O_3	25	5.0	298	—	1.13	19
Boehmite	2	5.0	298	—	0.73	19
Goethite	5	5.0	298	8.7	0.62	21
Hematite	7	5.0	298	8.4	0.67	20
Fe–Al–La	0.4	4.0	298	6.3	2.09	This study

favored for the adsorption of dissolved phytate onto the FAL adsorbent. A small proportion of dissolved phytate would likely be hydrolyzed to dissolved phosphate, especially under acidic conditions (Fig. 6c). Generally, the FAL adsorbent adsorbed much more phytate than dissolved phosphate at each pH. When the pH was >6.3, there would be fewer positive charges on the surface of the FAL adsorbent and greater OH^- in solution, where OH^- would compete with dissolved phytate and phosphate under alkaline conditions, which would result in lower capacities for adsorption of dissolved phytate.

3.5 Effect of coexisting anions and DOM on phytate adsorption

Coexisting anions such as Cl^-, NO_3^-, CO_3^{2-} and SO_4^{2-} are commonly distributed in natural and wastewaters. These coexisting anions would compete with phytate for active sites on the surface of the FAL adsorbent (Fig. 7). The capacities for adsorption of phytate onto the FAL adsorbent were inversely proportional to ionic strength increasing from 0 to 0.1 mol L^{-1}, which indicated that the adsorption was mainly due to outer-sphere (electrostatic) associations.[54] The strength of competition of coexisting anions with adsorption of phytate on the FAL adsorbent surface was in the order of $CO_3^{2-} > SO_4^{2-} > NO_3^- > Cl^-$. Generally, the effect of coexisting anions with two negative charges was stronger than that of coexisting anions with only one negative charge. Even 0.01 mol L^{-1} coexisting CO_3^{2-} and SO_4^{2-} anions could significantly reduce adsorption capacities. When the concentrations of coexisting CO_3^{2-} and SO_4^{2-} anions were 0.1 mol L^{-1}, the capacities for adsorption were 83.0% and 71.2% lower, respectively. In this study, the final pH of these solutions was near 4.0; thus, the surface charge of the FAL adsorbent was positive, which would adsorb coexisting anions. These resulted in the competition between phytate and coexisting anions. In particular, the coexisting CO_3^{2-} anion has a large negative charge and could bind to the metal active site through a bidentate inner-sphere bond.[55]

Table 4 Thermodynamic parameters for phytate adsorption onto the Fe–Al–La trimetal adsorbent

Temperature (K)	ΔG^0 (kJ mol^{-1})	ΔS^0 (J mol^{-1} K^{-1})	ΔH^0 (kJ mol^{-1})
298	−15.1	167.7	26.2
308	−20.4		
318	−29.4		

DOM is also a significant component and colloid in waste and natural waters, and influences the efficiency of adsorption capacities and biogeochemical cycling of nutrients in the environment such as in lakes.[41,56–58] HA is part of the labile organic matter pool in nature.[59] Meanwhile, Sigma-Aldrich HA is a technical humic acid extracted from lignite, and has been used as model labile organic matter for various environmental studies. Thus, as representative organic matter, the effect of HA on the adsorption capacity of phytate onto the FAL adsorbent was evaluated in this study (Fig. 8). The adsorption capacity (q_e) at the steady state was inversely proportional with the initial concentration of HA. Accordingly, the amount of HA adsorbed by the FAL adsorbent was greater at greater initial concentration of HA. These results indicated competition between phytate and HA on the surface of the FAL adsorbent. The prepared HA contained large amounts of functional groups, such as phenolic, carboxylic, amino, and alcoholic groups (Fig. 2), which would compete for adsorption with phytate.[34] Also, the adsorbed HA would likely generate an electrostatic field and negative charges, which could affect the capacity for adsorption of phytate onto the FAL adsorbent.[60]

3.6 Mechanisms of adsorption

The FAL adsorbent before and after phytate adsorption was characterized by FT-IR (Fig. 9). The FT-IR spectrum of the FAL adsorbent without phytate adsorption exhibited peaks at 3431, 1631, 1490, 1385, 1049, 835, and 570 cm^{-1} (Fig. 9a). The appearance of peaks at 3431 cm^{-1} and 1631 cm^{-1} was associated with the stretching and bending vibrations of H–O–H, which indicated physisorbed H_2O molecules on the surface of the prepared FAL adsorbent.[61] The peaks at 1490 cm^{-1} and 1385 cm^{-1} were assigned to La–OH,[62] while the peak at 1049 cm^{-1} was assigned to Fe–OH,[63] and the peak at 570 cm^{-1} was assigned to Al–O.[64] The characteristic peaks of the FAL adsorbent were weakened or shifted after adsorption of phytate from solutions, which indicated that Fe, Al, and La in the FAL adsorbent all participated in phytate adsorption. Also, after adsorption of phytate, four new peaks appeared at 1137, 1086, 993, and 668 cm^{-1} (Fig. 9b). The peak at 1137

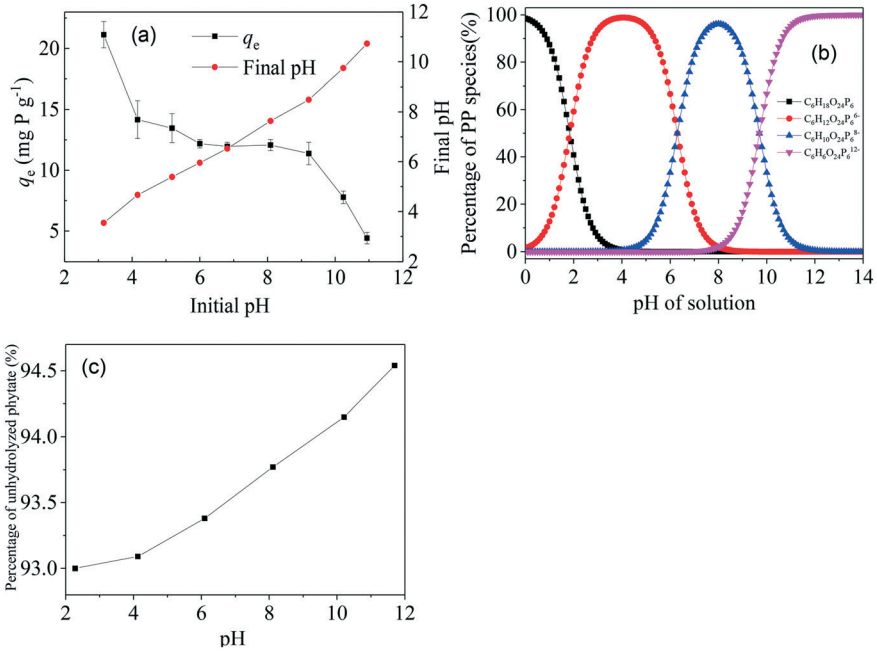

Fig. 6 Adsorption of phytate onto the Fe–Al–La trimetal adsorbent (a), species of dissolved phytate (b), and hydrolysis of dissolved phytate at different pH values (c).

cm^{-1} was associated with the stretching vibration bands of the P=O group.[65] The peak at 1086 cm^{-1} was assigned to the stretching vibration bands of P–O groups,[66] while the peak at 993 cm^{-1} was assigned to the bands of C–C stretching,[67] and the peak at 668 cm^{-1} was assigned to the bending vibration bands of O–P–O groups.[68] These results indicated that phytate had been adsorbed onto the surface of the prepared FAL adsorbent.

The FAL adsorbent after adsorption of phytate was further characterized by the use of XPS (Fig. 10). Elements, such as Fe, Al, La, O, C, and P, were characterized in the XPS spectrum, which further indicated that phytate was adsorbed onto the surface of the FAL adsorbent. Characteristic peaks of $FePO_4$, $LaPO_4$, and $AlPO_4$ were observed in the P2p XPS spectrum[69–71] (Fig. 10b). These results indicated that complexes were formed and Fe, Al, and La were all participating in phytate adsorption. The presence of characteristic peaks of $H_2PO_4^-$, HPO_4^{2-}, and PO_4^{3-} was likely due to hydrolysis of phytate (Fig. 6c). The characteristic peaks of C–C and C–O were identified at binding energies of 284.8 eV and 286.7 eV, respectively, in the C1s XPS spectrum.[72,73] These results further supported that phytate was adsorbed onto the FAL adsorbent.

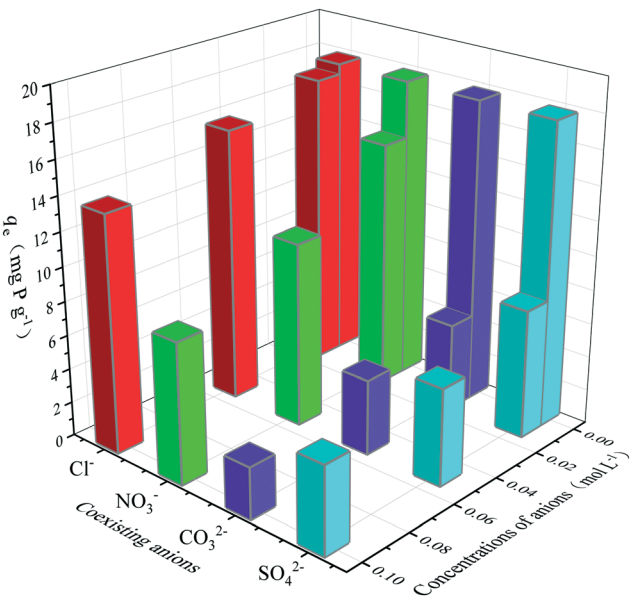

Fig. 7 Effect of coexisting anions on the adsorption of phytate onto the Fe–Al–La trimetal adsorbent.

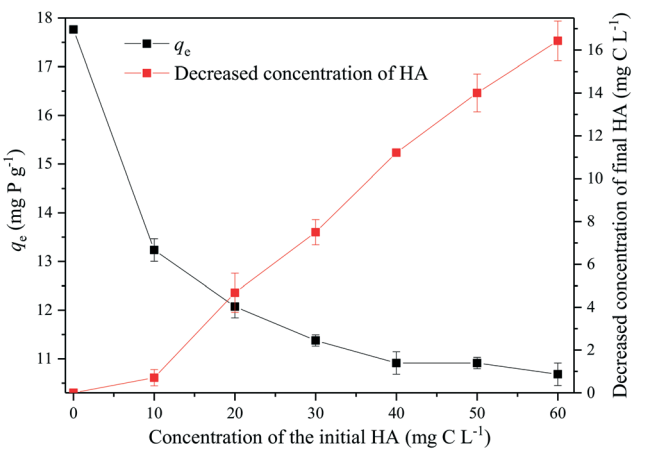

Fig. 8 Effect of HA on the adsorption of phytate by the Fe–Al–La trimetal adsorbent.

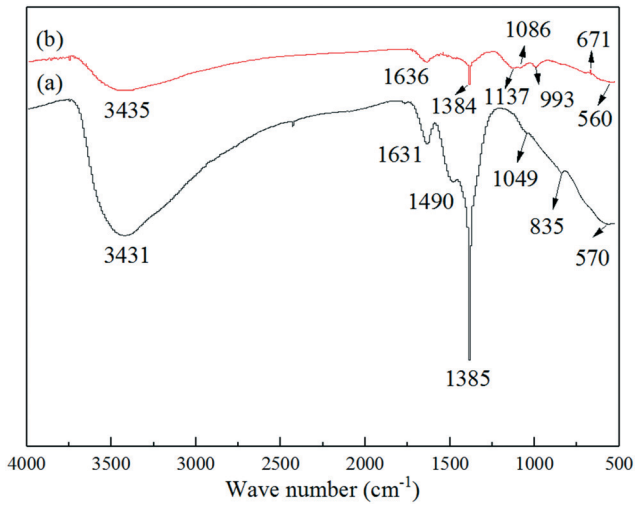

Fig. 9 FT-IR spectra of the Fe–Al–La trimetal adsorbent before (a) and after (b) adsorption by phytate.

The simultaneous adsorption of phosphate was also found when phytate was adsorbed by the FAL adsorbent. However, the adsorption of phosphate by the FAL adsorbent was not investigated simultaneously in this study. Based on a previous study of phosphate adsorption by a similar trimetal adsorbent (Fe–Mn–La trimetal composite adsorbent),[34] the adsorption kinetics, isotherms, and thermodynamics were all similar. However, the effects of pH, coexisting anions, organic matter on the adsorption of phytate and phosphate were different,[34] which implied that the adsorption mechanisms of phytate and phosphate were different. Generally, the organic moiety affected the process in terms of conformational hindrance; two to four phosphate groups of phytate were likely bound to Fe, Al oxides or other adsorbents.[19,24–26] Thus, the adsorption capacity, calculated by P, of phytate on the FAL adsorbent was likely 1.5 to 3 times higher than that of phosphate. However, Xu *et al.*[25] showed the maximum adsorption capacity of phytate, also calculated by P, by a La–Al hydroxide composite was

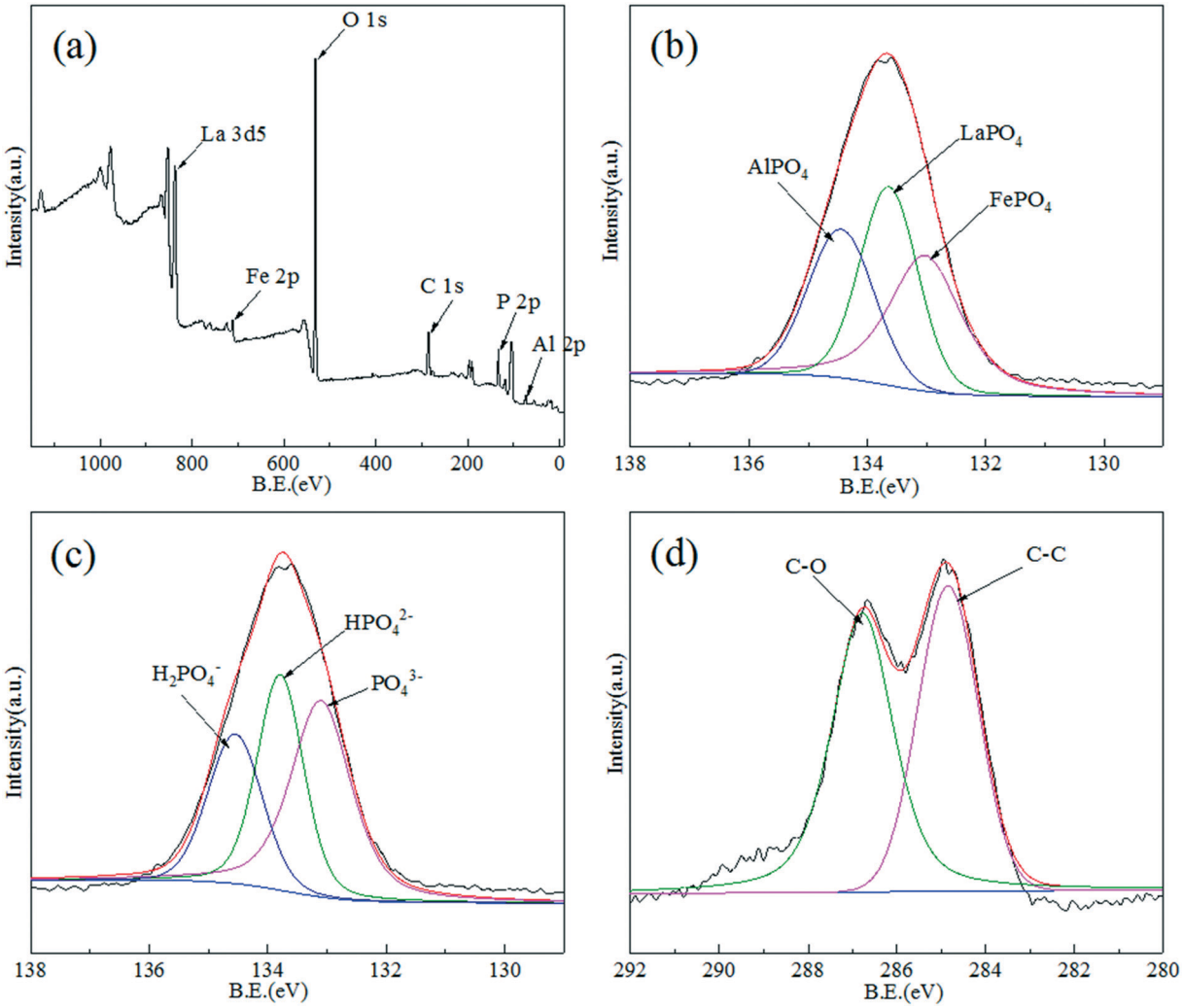

Fig. 10 XPS spectra of the Fe–Al–La trimetal adsorbent after phytate adsorption: (a) wide-scan XPS spectra, (b) and (c) P2p spectra, and (d) C1s spectra.

approximately 1.9 times lower than that of phosphate, which though that phytate has larger molecular dimensions and encounters increased steric hindrance than does phosphate. Thus, the different adsorption mechanisms of phytate and phosphate by the FAL adsorbent or other adsorbents should be investigated further.

3.7 Application and implications

Phytate is an organic phosphorus chemical found widely in natural environments, and can account for 60% to 80% of the phosphorus in mature seeds.[74] However, monogastric animals, such as pigs and poultry, cannot digest phytate, which results in excess phytate remaining in the manures of pig and poultry.[15,75] Thus, a rapid and cost effective method for treating phytate contained in wastewater containing pig and poultry manures was needed. It was found that such wastes could be effectively treated by the use of a FAL adsorbent to remove both phytate and phosphate.

Large amounts of phytate or phytate-like P have been found in sediments from some eutrophic lakes, such as Lake Dianchi[3] and Lake Taihu,[58] both of which are in China. However, the bioavailability of phytate from soils or sediments is still in dispute. It has been reported that phytate appeared to be stable in some sediments of lakes and could even be a phosphorus-specific paleoindicator.[76] However, long-term (20 years) application of phytate-rich poultry litter did not raise the organic P content in pasture soil, implying the lability of phytate and other organic P forms.[15] This observation has been further confirmed by various field and lab studies (*e.g.*, ref. 77–81). In this work, aggregate results showed that phytate adsorbed onto FAL adsorbents could be influenced by the amount of adsorbent, pH, and anion and DOM concentrations. Oxides of Al and Fe are key constituents involved in adsorption of phytate in sediments. Thus, the migration, transformation and bioavailability of phytate in sediments of lakes should be further elucidated. Eutrophication and blooming of algae can remove carbon dioxide and thus, increase the pH of the overlying water of lakes,[82,83] which are thus often alkaline with pH > 9.0 in eutrophic lakes such as Lake Dianchi, China.[83] When the pH exceeds 9.0, the phytate adsorbed onto the sediment is likely to be desorbed and released to the overlying water (Fig. 6a).

Eutrophication results in a rapid increase in DOM in lakes. The interaction of phytate and DOM such as HA and fulvic acid (FA) is an important factor influencing the bioavailability and preservation of phytate in sediments.[3,57,58,84] HA decreased the adsorption capacity of phytate on the FAL adsorbent, which also indicated that the increase in DOM would also likely decrease the adsorption of phytate by sediments or desorb phytate from sediments. Conversely, HA would also possibly interact with phytate to form HA-phytate or HA-metal-phytate complexes to resist hydrolysis by enzymes.[58,84] Thus, the comprehensive effect of DOM on the bioavailability of phytate in lakes should be clarified further. Generally, eutrophication of lakes could increase the amount of phytate as a bioavailable P source for algal blooms, such as those in Lake Dianchi.[3] The FAL adsorbent developed in this study could be a potential agent to immobilize both phytate and phosphate together in the overlying water and sediments of lakes.

4 Conclusions

A novel FAL trimetal composite adsorbent was developed for potential use in removing phytate by coprecipitation and showed a high adsorption capacity in a wide range of pH from 3.0 to 9.0. The removal efficiency at steady states was as much as 93%. Dynamic equilibrium was approached after 32 h. Adsorption kinetics were well described by pseudo-second-order kinetics. Adsorption isotherms were described well by the Langmuir model. The dominant process for adsorption of phytate onto the FAL adsorbent was surface chemical reactions which mainly occur in monolayers. Evaluation of the thermodynamic parameters indicated that the adsorption of phytate onto the FAL adsorbent was a spontaneous and endothermic process.

The adsorption capacity was proportional to the initial pH from 11.0 to 3.2, especially when pH > 9.0. The adsorption capacity was varied in a narrow range when the initial pH approached 4.0 to 9.0, which implied that the prepared FAL adsorbent could be well applied in a wide pH of wastewater or overlying water of lakes ranging from 3.0 to 9.0. The sequence of coexisting anions competing with phytate was $CO_3^{2-} > SO_4^{2-} > NO_3^- > Cl^-$. The presence of CO_3^{2-} would largely reduce the adsorption capacities of phytate onto the FAL adsorbent. DOM would also compete for the adsorption sites with phytate on the surface of the FAL adsorbent. Results of FT-IR and XPS analyses showed that the phytate was adsorbed onto the surface of the FAL adsorbent and that Fe, Al and La were all participating in adsorption. A small amount of orthophosphate hydrolyzed from phytate was also adsorbed onto the surface of the FAL adsorbent, which could be used for simultaneous removal of phytate and other phosphate species from wastewater, such as those from pig and poultry manures. The FAL adsorbent could also be used for immobilization of both phytate and phosphate in overlying water and sediments of lakes.

Conflicts of interest

The author(s) declared no potential conflicts of interest with respect to the research, authorship, and/or publication of this article.

Acknowledgements

This research was financially supported in part by the National Science Foundation of China (21777001, 41877380) and Key Research and Development Projects of Anhui Province (202004i07020006). Prof. Giesy was supported by the Canada Research Chair program, the 2012 "High Level Foreign Experts" (#GDT20143200016) program, funded by the State Administration of Foreign Experts Affairs, the P.R. China to Nanjing University and the Einstein Professor Program of

the Chinese Academy of Sciences and a Distinguished Visiting Professorship in the Department of Environmental Sciences, Baylor University in Waco, TX, USA.

References

1 D. J. Conley, H. W. Paerl, R. W. Howarth, D. F. Boesch, S. P. Seitzinger and K. E. Havens, *et al.*, Controlling eutrophication: nitrogen and phosphorus, *Science*, 2009, **323**, 1014–1015.
2 A. Paytan and K. McLaughlin, The Oceanic Phosphorus Cycle, *Chem. Rev.*, 2007, **107**, 563–576.
3 Y. Zhu, F. Wu, Z. He, J. Guo, X. Qu and F. Xie, *et al.*, Characterization of Organic Phosphorus in Lake Sediments by Sequential Fractionation and Enzymatic Hydrolysis, *Environ. Sci. Technol.*, 2013, **47**(14), 7679–7687.
4 V. H. Smith and D. W. Schindler, Eutrophication science: where do we go from here?, *Trends Ecol. Evol.*, 2009, **24**(4), 201–207.
5 J. Xie, Z. Wang, S. Lu, D. Wu, Z. Zhang and H. Kong, Removal and recovery of phosphate from water by lanthanum hydroxide materials, *Chem. Eng. J.*, 2014, **254**, 163–170.
6 P. J. Worsfold, P. Monbet, A. D. Tappin, M. F. Fitzsimons, D. A. Stiles and I. D. McKelvie, Characterisation and quantification of organic phosphorus and organic nitrogen components in aquatic systems: A Review, *Anal. Chim. Acta*, 2008, **624**(1), 37–58.
7 B. L. Turner, M. J. Papházy, P. M. Haygarth and I. D. McKelvie, Inositol phosphates in the environment, *Philos. Trans. R. Soc., B*, 2002, **357**(1420), 449–469.
8 P. Monbet, I. D. McKelvie, A. Saefumillah and P. J. Worsfold, A Protocol to Assess the Enzymatic Release of Dissolved Organic Phosphorus Species in Waters under Environmentally Relevant Conditions, *Environ. Sci. Technol.*, 2007, **41**(21), 7479–7485.
9 B. J. Cade-Menun, Characterizing phosphorus in environmental and agricultural samples by 31P nuclear magnetic resonance spectroscopy, *Talanta*, 2005, **66**(2), 359–371.
10 B. J. Cade-Menun, C. W. Liu, R. Nunlist and J. G. McColl, Soil and Litter Phosphorus-31 Nuclear Magnetic Resonance Spectroscopy, *J. Environ. Qual.*, 2002, **31**(2), 457–465.
11 J. E. Reusser, R. Verel, D. Zindel, E. Fr Ossard and T. I. Mclaren, Identification of lower-order inositol phosphates (IP5 and IP4) in soil extracts as determined by hypobromite oxidation and solution 31P NMR spectroscopy, *Biogeosciences*, 2019, **17**, 5079–5095.
12 B. L. Turner and A. E. Richardson, Identification scyllo-Inositol Phosphates in Soil by Solution Phosphorus-31 Nuclear Magnetic Resonance Spectroscopy, *Soil Sci. Soc. Am. J.*, 2004, **68**(3), 802–808.
13 J. V. Paraskova, C. Jørgensen, K. Reitzel, J. Pettersson, E. Rydin and P. J. R. Sjöberg, Speciation of Inositol Phosphates in Lake Sediments by Ion-Exchange Chromatography Coupled with Mass Spectrometry, Inductively Coupled Plasma Atomic Emission Spectroscopy, and 31P NMR Spectroscopy, *Anal. Chem.*, 2015, **87**(5), 2672–2677.
14 Z. He, Z. N. Senwo, R. N. Mankolo and C. W. Honeycutt, Phosphorus fractions in poultry litter characterized by sequential fractionation coupled with phosphatase hydrolysis, *J. Food, Agric. Environ.*, 2006, **4**(1), 304–312.
15 Z. He, C. W. Honeycutt, B. J. Cade-Menun, Z. N. Senwo and I. A. Tazisong, Phosphorus in Poultry Litter and Soil: Enzymatic and Nuclear Magnetic Resonance Characterization, *Soil Sci. Soc. Am. J.*, 2008, **72**, 1425–1433.
16 Z. He, J. Zhong and H. N. Cheng, Conformational change of metal phytates: Solid state 1D 13C and 2D 1H-13C NMR spectroscopic investigations, *J. Food, Agric. Environ.*, 2013, **11**(1), 965–970.
17 Z. He, C. W. Honeycutt, T. Zhang and P. M. Bertsch, Preparation and FT-IR characterization of metal phytate compounds, *J. Environ. Qual.*, 2006, **35**(4), 1319–1328.
18 Y. Yan, L. K. Koopal, W. Li, A. Zheng, J. Yang and F. Liu, *et al.*, Size-dependent sorption of myo-inositol hexakisphosphate and orthophosphate on nano-γ-Al_2O_3, *J. Colloid Interface Sci.*, 2015, **451**, 85–92.
19 Y. Yan, W. Li, J. Yang, A. Zheng, F. Liu and X. Feng, *et al.*, Mechanism of Myo-inositol Hexakisphosphate Sorption on Amorphous Aluminum Hydroxide: Spectroscopic Evidence for Rapid Surface Precipitation, *Environ. Sci. Technol.*, 2014, **48**(12), 6735–6742.
20 Y. Yan, B. Wan, F. Liu, W. Tan, M. Liu and X. Feng, Adsorption-Desorption of Myo-Inositol Hexakisphosphate on Hematite, *Soil Sci.*, 2014, **179**(10–11), 476–485.
21 Y. Yan, L. K. Koopal, F. Liu, Q. Huang and X. Feng, Desorption of myo-inositol hexakisphosphate and phosphate from goethite by different reagents, *J. Plant Nutr. Soil Sci.*, 2015, **178**(6), 878–887.
22 L. Celi, G. D. Luca and E. Barberis, Effects of interaction of organic and inorganic P with ferrihydrite and kaolinite-iron oxide systems on iron release, *Soil Sci.*, 2003, **168**(7), 479–488.
23 Z. Hu, D. P. Jaisi, Y. Yan, H. Chen, X. Wang and B. Wan, *et al.*, Adsorption and precipitation of myo-inositol hexakisphosphate onto kaolinite, *Eur. J. Soil Sci.*, 2020, **71**(2), 226–235.
24 F. Qiu, J. Wang, D. Zhao and K. Fu, Adsorption of myo-inositol hexakisphosphate in water using recycled water treatment residual, *Environ. Sci. Pollut. Res.*, 2018, **25**(29), 29593–29604.
25 R. Xu, T. Lyu, M. Zhang, M. Cooper and G. Pan, Molecular-level investigations of effective biogenic phosphorus adsorption by a lanthanum/aluminum-hydroxide composite, *Sci. Total Environ.*, 2020, **725**, 138424.
26 X. Wang, Y. Hu, Y. Tang, P. Yang, X. Feng and W. Xu, *et al.*, Phosphate and phytate adsorption and precipitation on ferrihydrite surfaces, *Environ. Sci.: Nano*, 2017, **4**(11), 2193–2204.
27 B. Wan, Y. P. Yan, M. Q. Zhu, X. M. Wang, F. Liu and W. F. Tan, *et al.*, Quantitative and spectroscopic investigations of the co-sorption of myo-inositol hexakisphosphate and

cadmium(II) on to haematite, *Eur. J. Soil Sci.*, 2017, **68**(3), 374–383.

28 Y. Yan, B. Wan, D. P. Jaisi, H. Yin, Z. Hu and X. Wang, *et al.*, Effects of Myo-inositol Hexakisphosphate on Zn(II) Sorption on γ-Alumina: A Mechanistic Study, *ACS Earth Space Chem.*, 2018, **2**(8), 787–796.

29 C. Shang, J. Stewart and P. M. Huang, pH effect on kinetics of adsorption of organic and inorganic phosphates by short-range ordered aluminum and iron precipitates, *Geoderma*, 1992, **53**(1–2), 1–14.

30 Y. Hu, M. Zhu, X. Wang, X. Feng, Y. Tang and W. Xu, *et al.*, Phosphate and phytate adsorption and precipitation on ferrihydrite surfaces, *Environ. Sci.: Nano*, 2017, **4**(11), 2193–2204.

31 C. J. De Groot and H. L. Golterman, On the presence of organic phosphate in some Camargue sediments: evidence for the importance of phytate, *Hydrobiologia*, 1993, **252**(1), 117–126.

32 C. Jørgensen, H. S. Jensen, F. Ø. Andersen, S. Egemose and K. Reitzel, Occurrence of orthophosphate monoesters in lake sediments: significance of myo-and scyllo-inositol hexakisphosphate, *J. Environ. Monit.*, 2011, **13**(8), 2328–2334.

33 Z. He, P. H. Pagliari and H. M. Waldrip, Applied and Environmental Chemistry of Animal Manure:A Review, *Pedosphere*, 2016, **26**(06), 779–816.

34 Y. Zhu, X. Yue and F. Xie, Adsorptive removal of phosphate by a Fe–Mn–La tri-metal composite sorbent: Adsorption capacity, influence factors, and mechanism, *Adsorpt. Sci. Technol.*, 2020, **38**(7–8), 254–270.

35 Z. Hussain, L. Daosheng, L. Xi and K. Jianxiong, Defluoridation by a Mg–Al–La triple-metal hydrous oxide: synthesis, sorption, characterization and emphasis on the neutral pH of treated water, *RSC Adv.*, 2015, **5**(55), 43906–43916.

36 J. Wang, L. Wu, J. Li, D. Tang and G. Zhang, Simultaneous and efficient removal of fluoride and phosphate by Fe-La composite: Adsorption kinetics and mechanism, *J. Alloys Compd.*, 2018, **753**, 422–432.

37 J. Wang, D. Kang, X. Yu, M. Ge and Y. Chen, Synthesis and characterization of Mg–Fe–La trimetal composite as an adsorbent for fluoride removal, *Chem. Eng. J.*, 2015, **264**, 506–513.

38 Y. Yu and C. J. Paul, Key factors for optimum performance in phosphate removal from contaminated water by a Fe–Mg–La tri-metal composite sorbent, *J. Colloid Interface Sci.*, 2015, **445**, 303–311.

39 Y.-T. Liu and D. Hesterberg, Phosphate Bonding on Noncrystalline Al/Fe-Hydroxide Coprecipitates, *Environ. Sci. Technol.*, 2011, **45**(15), 6283–6289.

40 J. Murphy and J. P. Riley, A modified single solution method for the determination of phosphate in natural waters, *Anal. Chim. Acta*, 1962, **27**, 31–36.

41 F. Xie, Z. Dai, Y. Zhu, G. Li, H. Li and Z. He, *et al.*, Adsorption of phosphate by sediments in a eutrophic lake: Isotherms, kinetics, thermodynamics and the influence of dissolved organic matter, *Colloids Surf., A*, 2019, **562**, 16–25.

42 J. Wang, J. Xu, J. Xia, F. Wu and Y. Zhang, A kinetic study of concurrent arsenic adsorption and phosphorus release during sediment resuspension, *Chem. Geol.*, 2018, **495**, 67–75.

43 H. N. Tran, S.-J. You, A. Hosseini-Bandegharaei and H.-P. Chao, Mistakes and inconsistencies regarding adsorption of contaminants from aqueous solutions: A critical review, *Water Res.*, 2017, **120**, 88–116.

44 M. Zhang and Z. He, Characteristics of Dissolved Organic Carbon Revealed by Ultraviolet-Visible Absorbance and Fluorescence Spectroscopy: The Current Status and Future Exploration, *Labile Organic Matter—Chemical Compositions, Function, and Significance in Soil and the Environment*, 2015, pp. 1–21.

45 L. Doskočil, J. Burdíková-Szewieczková, V. Enev, L. Kalina and J. Wasserbauer, Spectral characterization and comparison of humic acids isolated from some European lignites, *Fuel*, 2018, **213**, 123–132.

46 Z. He and M. Zhang, Structural and Functional Comparison of Mobile and Recalcitrant Humic Fractions from Agricultural Soils, *Labile Organic Matter—Chemical Compositions, Function, and Significance in Soil and the Environment*, 2015, pp. 79–98.

47 Z. He, T. Ohno, B. J. Cade-Menun, M. S. Erich and C. W. Honeycutt, Spectral and Chemical Characterization of Phosphates Associated with Humic Substances, *Soil Sci. Soc. Am. J.*, 2006, **70**(5), 1741–1751.

48 P. Xia, X. Wang, X. Wang, J. Song, H. Wang and J. Zhang, *et al.*, Struvite crystallization combined adsorption of phosphate and ammonium from aqueous solutions by mesoporous MgO loaded diatomite, *Colloids Surf., A*, 2016, **506**, 220–227.

49 J. Lü, H. Liu, R. Liu, X. Zhao, L. Sun and J. Qu, Adsorptive removal of phosphate by a nanostructured Fe–Al–Mn trimetal oxide adsorbent, *Powder Technol.*, 2013, **233**, 146–154.

50 P. Chen, T. Wang, Y. Xiao, E. Tian, W. Wang and Y. Zhao, *et al.*, Efficient fluoride removal from aqueous solution by synthetic Fe-Mg-La tri-metal nanocomposite and the analysis of its adsorption mechanism, *J. Alloys Compd.*, 2018, **738**, 118–129.

51 Z. Ajmal, A. Muhmood, M. Usman, S. Kizito, J. Lu and R. Dong, *et al.*, Phosphate removal from aqueous solution using iron oxides: Adsorption, desorption and regeneration characteristics, *J. Colloid Interface Sci.*, 2018, **528**, 145–155.

52 L.-G. Yan, Y.-Y. Xu, H.-Q. Yu, X.-D. Xin, Q. Wei and B. Du, Adsorption of phosphate from aqueous solution by hydroxy-aluminum, hydroxy-iron and hydroxy-iron–aluminum pillared bentonites, *J. Hazard. Mater.*, 2010, **179**(1), 244–250.

53 S. S. Tripathy, J.-L. Bersillon and K. Gopal, Removal of fluoride from drinking water by adsorption onto alum-impregnated activated alumina, *Sep. Purif. Technol.*, 2006, **50**(3), 310–317.

54 M. B. McBride, A critique of diffuse double layer models applied to colloid and surface chemistry, *Clays Clay Miner.*, 1997, **45**(4), 598–608.

55 L. Zhang, Y. Gao, Y. Xu and J. Liu, Different performances and mechanisms of phosphate adsorption onto metal oxides and metal hydroxides: a comparative study, *J. Chem. Technol. Biotechnol.*, 2016, **91**(5), 1232–1239.
56 F. Wu and B. Xing, *Natural Organic Matter and Its significance in the Environment*, Science Press, Beijing, 2009.
57 Y. Zhu, F. Wu, W. Feng, S. Liu and J. P. Giesy, Interaction of alkaline phosphatase with minerals and sediments: Activities, kinetics and hydrolysis of organic phosphorus, *Colloids Surf., A*, 2016, **495**, 46–53.
58 Y. Zhu, F. Wu, Z. He, J. P. Giesy, W. Feng and Y. Mu, *et al.*, Influence of Natural Organic Matter on the Bioavailability and Preservation of Organic Phosphorus in Lake Sediments, *Chem. Geol.*, 2015, **397**, 51–60.
59 Z. He and F. Wu, *Labile Organic Matter: Chemical Compositions, Function, and Significance in Soil and the Environment*, SSSA Special Publication 62, Soil Science Society of America, Madison, Wisconsin, 2015.
60 Z. Fu, F. Wu, K. Song, Y. Lin, Y. Bai and Y. Zhu, *et al.*, Competitive interaction between soil-derived humic acid and phosphate on goethite, *Appl. Geochem.*, 2013, **36**, 125–131.
61 L. Li, Q. Zhu, K. Man and Z. Xing, Fluoride removal from liquid phase by Fe-Al-La trimetal hydroxides adsorbent prepared by iron and aluminum leaching from red mud, *J. Mol. Liq.*, 2017, **237**, 164–172.
62 W. Zhang, J. Fu, G. Zhang and X. Zhang, Enhanced arsenate removal by novel Fe-La composite (hydr)oxides synthesized via coprecipitation, *Chem. Eng. J.*, 2014, **251**(251), 69–79.
63 J. Lu, D. Liu, J. Hao, G. Zhang and B. Lu, Phosphate removal from aqueous solutions by a nano-structured Fe–Ti bimetal oxide sorbent, *Chem. Eng. Res. Des.*, 2015, **93**, 652–661.
64 W. Xiang, G. Zhang, Y. Zhang, D. Tang and J. Wang, Synthesis and characterization of cotton-like Ca–Al–La composite as an adsorbent for fluoride removal, *Chem. Eng. J.*, 2014, **250**, 423–430.
65 J. Song, Z. Yu, M. L. Gordin, S. Hu, R. Yi and D. Tang, *et al.*, Chemically Bonded Phosphorus/Graphene Hybrid as a High Performance Anode for Sodium-Ion Batteries, *Nano Lett.*, 2014, **14**(11), 6329–6335.
66 M. C. Zenobi, C. V. Luengo, M. J. Avena and E. H. Rueda, An ATR-FTIR study of different phosphonic acids adsorbed onto boehmite, *Spectrochim. Acta, Part A*, 2010, **75**(4), 1283–1288.
67 J. Titus, C. Filfili, A. Perera and J. K. Hilliard, Inventors Early detection of cell activation by ATR-FTIR spectroscopy patent, *US Pat.*, 9983129, 2018.
68 S. Chandrawanshi, S. K. Verma and M. K. Deb, Ion-pair single-drop microextraction with ATR-FTIR determination of phosphate in water samples, *Indian J. Chem., Sect. A: Inorg., Bio-inorg., Phys., Theor. Anal. Chem.*, 2018, **57**(2), 168–174.
69 X. Wu, K. Gong, G. Zhao, W. Lou, X. Wang and W. Liu, Mechanical synthesis of chemically bonded phosphorus–graphene hybrid as high-temperature lubricating oil additive, *RSC Adv.*, 2018, **8**(9), 4595–4603.
70 A. T. Appapillai, A. N. Mansour, J. Cho and Y. Shao-Horn, Microstructure of $LiCoO_2$ with and without "$AlPO_4$" Nanoparticle Coating: Combined STEM and XPS Studies, *Chem. Mater.*, 2007, **19**(23), 5748–5757.
71 Z. Wang, D. Shen, F. Shen and T. Li, Phosphate adsorption on lanthanum loaded biochar, *Chemosphere*, 2016, **150**, 1–7.
72 R. Mccann, S. S. Roy, P. Papakonstantinou, M. F. Bain, H. S. Gamble and J. A. Mclaughlin, Chemical bonding modifications of tetrahedral amorphous carbon and nitrogenated tetrahedral amorphous carbon films induced by rapid thermal annealing, *Thin Solid Films*, 2005, **482**(1/2), 34–40.
73 Y. Zhu, G. Wu, Y.-H. Zhang and Q. Zhao, Growth and characterization of $Mg(OH)_2$ film on magnesium alloy AZ31, *Appl. Surf. Sci.*, 2011, **257**(14), 6129–6137.
74 V. Raboy, Seed phosphorus and the development of low-phytate crops, ed. B. L.Turner, A. E. Richardson and E. J. Mullaney, in: *Inositol Phosphates Linking Agriculture & the Environment*, CABI, 2006, pp. 111–132.
75 Z. He, B. J. Cade-Menun, G. S. Toor, A. M. Fortuna, C. W. Honeycutt and J. T. Sims, Comparison of Phosphorus Forms in Wet and Dried Animal Manures by Solution Phosphorus-31 Nuclear Magnetic Resonance Spectroscopy and Enzymatic Hydrolysis, *J. Environ. Qual.*, 2007, **36**, 1086–1095.
76 B. L. Turner and K. Weckström, Phytate as a novel phosphorus-specific paleo-indicator in aquatic sediments, *J. Paleolimnol.*, 2009, **42**(3), 391–400.
77 A. L. Doolette, R. J. Smernik and W. J. Dougherty, Overestimation of the importance of phytate in NaOH-DTA soil extracts as assessed by ^{31}P NMR analyses, *Org. Geochem.*, 2011, **42**(8), 955–964.
78 K. E. Annaheim, A. L. Doolette, R. J. Smernik, J. Mayer, A. Oberson and E. Frossard, *et al.*, Long-term addition of organic fertilizers has little effect on soil organic phosphorus as characterized by 31P NMR spectroscopy and enzyme additions, *Geoderma*, 2015, **257–258**, 67–77.
79 M. Keller, A. Oberson, K. E. Annaheim, F. Tamburini, P. Mäder and J. Mayer, *et al.*, Phosphorus forms and enzymatic hydrolyzability of organic phosphorus in soils after 30 years of organic and conventional farming, *J. Plant Nutr. Soil Sci.*, 2012, **175**, 385–393.
80 I. A. Tazisong, Z. N. Senwo, B. J. Cade-Menun and Z. He, Phosphorus Forms and Mineralization Potentials of Alabama Upland Cotton Production Soils Amended with Poultry Litter, in: *Applied Manure and Nutrient Chemistry for Sustainable Agriculture and Environment*, ed. Z. He and H. Zhang, Springer Netherlands, Dordrecht, 2014, pp. 191–209.
81 H. Waldrip-Dail, Z. He, S. M. Erich and W. C. Honeycutt, Soil Phosphorus Dynamics in Response to Poultry Manure Amendment, *Soil Sci.*, 2009, **174**(4), 195–201.
82 J. B. Thompson and F. G. Ferris, Cyanobacterial precipitation of gypsum, calcite, and magnesite from natural alkaline lake water, *Geology*, 1990, **18**(10), 992–998.
83 X. Cao, Y. Wang, J. He, X. Luo and Z. Zheng, Phosphorus mobility among sediments, water and cyanobacteria enhanced by cyanobacteria blooms in eutrophic Lake Dianchi, *Environ. Pollut.*, 2016, **219**, 580–587.

84 Y. Zhu, W. Feng, S. Liu, Z. He, X. Zhao and Y. Liu, *et al.*, Bioavailability and preservation of organic phosphorus in lake sediments: Insights from enzymatic hydrolysis and 31P nuclear magnetic resonance, *Chemosphere*, 2018, **211**, 50–61.